AGU PUBLICATIONS

JGR

Journal of Geophysical Research: Oceans

RESEARCH ARTICLE

10.1002/2015JC011433

Key Points:
- Arctic Ocean albedo modification offsets Arctic climate trends only temporarily
- Compensatory oceanic heat fluxes result in an Arctic Ocean subsurface warming
- On longer time scales emission reduction is more effective in staying close to today's climate state

Supporting Information:
- Supporting Information S1

Correspondence to:
N. Mengis,
nmengis@geomar.de

Citation:
Mengis, N., T. Martin, D. P. Keller, and A. Oschlies (2016), Assessing climate impacts and risks of ocean albedo modification in the Arctic, *J. Geophys. Res. Oceans*, *121*, doi:10.1002/2015JC011433.

Received 3 NOV 2015
Accepted 7 APR 2016
Accepted article online 12 APR 2016

Assessing climate impacts and risks of ocean albedo modification in the Arctic

N. Mengis[1], T. Martin[1], D. P. Keller[1], and A. Oschlies[1,2]

[1]Helmholtz Centre for Ocean Research Kiel (GEOMAR), Kiel, Germany, [2]Kiel University, Kiel, Germany

Abstract The ice albedo feedback is one of the key factors of accelerated temperature increase in the high northern latitudes under global warming. This study assesses climate impacts and risks of idealized Arctic Ocean albedo modification (AOAM), a proposed climate engineering method, during transient climate change simulations with varying representative concentration pathway (RCP) scenarios. We find no potential for reversing trends in all assessed Arctic climate metrics under increasing atmospheric CO_2 concentrations. AOAM only yields an initial offset during the first years after implementation. Nevertheless, sea ice loss can be delayed by 25(60) years in the RCP8.5(RCP4.5) scenario and the delayed thawing of permafrost soils in the AOAM simulations prevents up to 40(32) Pg of carbon from being released by 2100. AOAM initially dampens the decline of the Atlantic Meridional Overturning and delays the onset of open ocean deep convection in the Nordic Seas under the RCP scenarios. Both these processes cause a subsurface warming signal in the AOAM simulations relative to the default RCP simulations with the potential to destabilize Arctic marine gas hydrates. Furthermore, in 2100, the RCP8.5 AOAM simulation diverts more from the 2005–2015 reference state in many climate metrics than the RCP4.5 simulation without AOAM. Considering the demonstrated risks, we conclude that concerning longer time scales, reductions in emissions remain the safest and most effective way to prevent severe changes in the Arctic.

1. Introduction

Over the last decades air temperatures have been rising much faster in the Arctic than in other regions of the planet [*Screen Simmonds*, 2010]. This Arctic amplification of global warming is strongly connected to positive feedback mechanisms [*Stocker et al*., 2013; *Serreze and Francis*, 2006], with the ice albedo feedback being of special importance [*Holland and Bitz*, 2003]. Positive feedbacks can amplify the consequences and spatial impact of an initially local perturbation. While our scientific understanding of feedback processes of the Earth system is still far from complete, currently the Arctic is perceived as a system that holds tipping points of relevance for the global climate [*Lenton et al*., 2008; *Lenton*, 2012]. However, the existence of such tipping points especially concerning Arctic sea ice has been challenged and is under debate [e.g., *Tietsche et al*., 2011; *Wadhams*, 2012]. Six of 15 policy-relevant potential future tipping elements discussed by *Lenton et al*. [2008] are located in the high northern latitudes: (i) the risk of Arctic summer sea ice loss, (ii) the break down of Atlantic deep water formation and an associated slowing down of the meridional overturning circulation (MOC), (iii) permafrost thawing and consequently a release of carbon and methane from the soils, (iv) a destabilization of marine methane hydrates, (v) the melt and collapse of the Greenland ice sheet, and (vi) the development of an Arctic ozone hole.

With global CO_2 emissions still increasing and climate change progressing [*Stocker et al*., 2013], there is more and more interest in technological approaches that would counteract climate change. A number of so-called Climate Engineering (CE) methods have been suggested [*Crutzen*, 2006]. They can be partitioned into carbon dioxide removal methods, aimed at reducing atmospheric CO_2 concentrations, and solar radiation management (SRM) methods, aimed at manipulating the Earth's radiation budget without addressing atmospheric CO_2 concentrations. For both CE methods implementation and governance concepts are discussed widely [e.g., *Robock*, 2008; *Blackstock et al*., 2009; *Feichter and Leisner*, 2009; *Keith*, 2013; *Hulme*, 2014].

Because of the already progressing large anthropogenic warming signal in the Arctic, the expected future warming threats, and the regionally relatively confined atmospheric and oceanographic circulation features, the Arctic is of particular interest when it comes to debating regional-scale interventions in the climate

system. Most of the previous studies on the impact of Arctic CE investigate atmospheric SRM by either dimming the incoming short wave radiation [*Caldeira and Wood*, 2008; *MacCracken et al*., 2013; *Tilmes et al*., 2013] or by explicitly modeling the implementation of sulphate aerosols in the high northern latitudes [*Robock et al*., 2008]. The focus of these studies was set predominately on CE impacts on atmospheric metrics, such as surface temperature and precipitation [*Caldeira and Wood*, 2008; *Robock et al*., 2008]. *Tilmes et al*. [2013] additionally investigated changes in atmospheric as well as oceanic heat transports. Recently, *Cvijanovic et al*. [2015] investigated the potential of ocean albedo modification on Arctic sea ice restoration and climate in a model set up of an abrupt quadrupling of CO_2. They found that a constant albedo of 0.9 applied to the area north of 70°N or 75°N was most effective in restoring Arctic sea ice, with September sea ice area stabilizing at about 40% of preindustrial sea ice coverage in both idealized scenarios. They did not investigate possible impacts on ocean heat content or ocean circulation however. In the current study, we investigate modifications of the ocean surface albedo at high northern latitudes during transient climate change under 21st century Coupled Model Intercomparison Project 5 (CMIP5) [*Taylor et al*., 2012] emission scenarios, with special emphasis of changes in ocean heat content and meridional overturning circulation.

Holland and Bitz [2003] state that the ice albedo feedback is one of the key factors of the positive feedback mechanisms, which amplify climate change in the high northern latitudes. Open water has an albedo of 0.03–0.4 [*Jin et al*., 2004], whereas the albedo of sea ice ranges between 0.6 and 0.7 for bare ice and 0.8–0.9 for snow-covered ice [*Perovich et al*., 2002]. The CE approach studied here aims to exploit this feedback by implementing an albedo modification on ice-free ocean areas in summer. Arctic amplification of global warming is strongest in autumn and winter [*Serreze and Barry*, 2011], which is the season when the ocean releases the heat absorbed over summer to the atmosphere. Larger ice-free areas in summer enable more oceanic heat storage and a larger heat release to the atmosphere in autumn and winter. Therefore, the objective of this CE approach is to increase ocean surface albedo, reducing energy absorption by the ocean, and thus limiting the heat exchange with the atmosphere during summer and fall. This approach is expected to limit the sea ice loss in summer and foster the formation and maintenance of a multiyear ice cover in the long term.

Suggestion on possible implementation schemes for an artificial surface albedo modification include the use of oceanic foams [*Evans et al*., 2010], microbubbles [*Seitz*, 2011] in combination with surfactants [*Crook et al*., 2016], or floating glass spheres [*Gordon and Walter*, 2011]. However, a detailed discussion of the technical aspects of deployment is beyond the scope of this paper. We focus on modeling potential consequences of an assumed successful implementation, using an ocean-sea ice model coupled to a simple atmospheric model and a global carbon cycle model, in order to investigate an idealized albedo modification over the Arctic Ocean surface.

This study is organized as follows: Section 2 describes the model implementation of the CE approach. In section 3 we present the results of our study, whereby the above mentioned potential tipping elements in the Earth system of *Lenton et al*. [2008] are used as a guideline for the analysis. Section 4 includes a general discussion and the conclusion is presented in section 5.

2. Methods

2.1. Model Description

The model employed is the University of Victoria Earth System Climate Model (UVic ESCM) version 2.9, an Earth system model of intermediate complexity [*Weaver et al*., 2001; *Eby et al*., 2013]. It includes schemes for ocean physics based on the Modular Ocean Model Version 2 (MOM2) [*Pacanowski*, 1995], ocean biogeochemistry [*Keller et al*., 2012], and a terrestrial component including soil and vegetation dynamics [*Meissner et al*., 2003]. It is coupled to a dynamic-thermodynamic sea ice model with several ice thickness categories [*Bitz et al*., 2001] and elastic visco-plastic rheology [*Hunke and Dukowicz*, 1997]. The atmosphere is represented by a two dimensional atmospheric energy moisture balance model [*Fanning and Weaver*, 1996]. Note, that *Skvortsov et al*. [2009] positively evaluated the UVic ESCM for surface air temperature as well as snow cover in the Arctic. All model components have a common horizontal resolution of 3.6° longitude and 1.8° latitude and the oceanic component has a vertical resolution of 19 levels, with vertical thickness varying between 50 m near the surface to 500 m in the deep ocean.

Wind velocities used to calculate advection of atmospheric heat and moisture as well as the air-sea ice exchange of surface momentum, is prescribed as monthly climatological wind fields from NCAR/NCEP reanalysis data [*Keller et al*., 2014]. The planetary albedo varies as a function of latitude and time of year to account for changes in solar zenith angle. Atmospheric albedo, representing clouds and aerosols, are prescribed monthly fields held constant throughout the simulations. The surface albedo in the model depends on the vegetation and snow coverage over land areas and on the sea ice coverage over the ocean, where the default sea ice albedo has a value of 0.8 (see supporting information Figure S1 for the reference model surface albedo distribution in 2005).

2.2. Experimental Set Up and Forcing

The UVic ESCM was spun up with preindustrial (year 1800) seasonally varying forcing for over 10,000 years. All simulations were integrated from 1765 until 2005 using historical fossil-fuel and land-use carbon emissions, as well as radiative forcing from solar variability and volcanic activity. Historical land use changes were implemented following the protocols of the CMIP5. Following *Keller et al*. [2014], continental ice sheets were held constant to facilitate the experimental setting and analyses. Branching off from the control simulation in 2005, three default experiments running until 2100 were conducted. Two follow the CO_2 emission scenarios of the Representative Concentration Pathways (RCPs) 8.5 and 4.5 from *Meinshausen et al*. [2011] and one features no CO_2 emission from 2005 onward (noEmit). The latter represents an idealized maximum mitigation scenario (disregarding the possibility of negative emissions). Note, that there is a concomitant warming and associated further reduction in sea ice even in this simulation due to the CO_2 that is already emitted until 2005, a large portion of which remains in the atmosphere until the end of the simulation.

For each of these three scenarios we ran an additional simulation with Arctic Ocean Albedo Modification (AOAM) starting in 2020. AOAM is implemented by prescribing a surface albedo of 0.8, i.e., the model's default value for sea ice, whenever the sea ice concentration drops below 50% in grid cells north of 70°N (Figure 1). This is done for every model time step from 2020 to 2100. Note, that AOAM only affects the incoming shortwave fluxes directly. Atmosphere-ocean heat fluxes, longwave fluxes and evaporative fluxes may change due to interactive physical processes. If a specific implementation method were to be tested, the model implementation would need to be adjusted. For example, if we considered the implementation of microbubbles, this would in addition to surface albedo also affect evaporative fluxes. For diagnostic purposes, a virtual tracer that is analogous to adding an inert dye to water was implemented in the whole Arctic basin north of 70°N over all depth levels, where it was set to the value 1, at the beginning of the experiment in 2020. The tracer allowed us to track the pathways of the water masses entering and leaving the Arctic Ocean (for more details on the tracer evaluation, see section A in the supporting information).

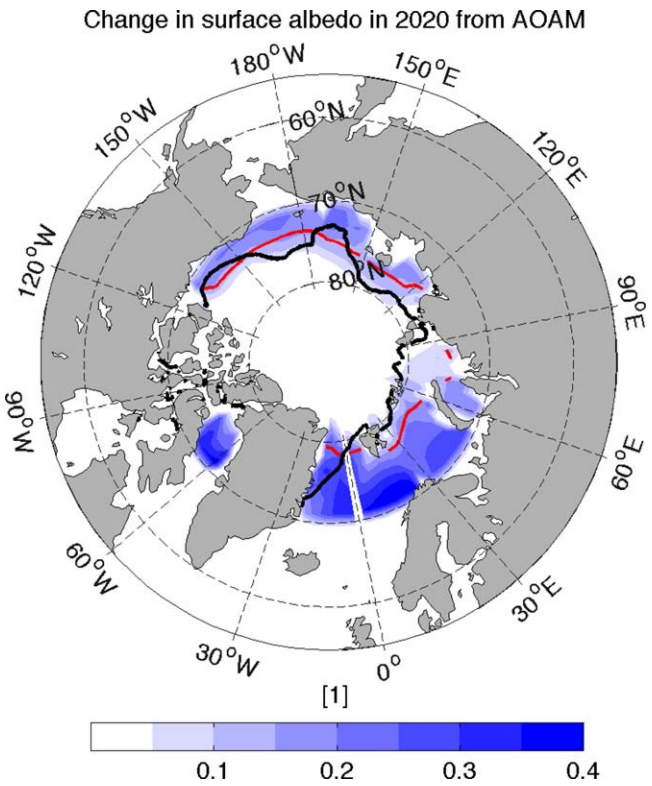

Figure 1. Annual mean changes in surface albedo in the Arctic due to the AOAM implementation in 2020 exemplarily in the RCP8.5 scenarios, i.e., RCP8.5 AOAM minus RCP8.5. As a reference the mean september sea ice edge defined as the 15% sea ice concentration contour line from observations (black line) and the UVic ESCM (red line) for the period of 2005–2014 is shown, where observations are taken from *Meier et al*. [2013].

For all emission scenarios, the annual maximum area over which AOAM is applied in 2020 is about 5.1 million km^2 (Figure 1). By the end of the century, for simulations with increasing CO_2 emissions, the maximum AOAM area increased to 7.8 (5.8) million km^2 for the RCP8.5 (RCP4.5) simulation during summer times. These areas account for 77 (58) % of the oceanic Arctic area north of 70°N. For the noEmit simulation, the maximum AOAM area in the summers of 2090–2100 has slightly decreased to 4.3 million km^2, which amounts to 42% of the Arctic Ocean area. The fact that the area of implementation is increasing with time for the two scenarios with increasing atmospheric CO_2 concentrations already indicates a loss in summer Arctic sea ice, regardless of the implemented albedo modification, and hints at the enormous technical challenge of maintaining AOAM over time in reality.

The objective of AOAM is to alter the radiation budget at the Arctic Ocean surface by mimicking an initiation of the ice-albedo effect, one of the key factors for Arctic amplification of climate change [*Holland and Bitz*, 2003]. Other feedbacks, such as the cloud-albedo feedback [*Serreze and Barry*, 2011] are not included in the simulations, since the UVic ESCM simulates no change of cloud albedo with time. This neglected cloud response might lead to a bias in the simulated effect of AOAM.

3. Results

For both, the RCP8.5 and RCP4.5, emission scenarios, the global impact of simulated AOAM is small compared to the reference global annual mean surface air temperature changes of 2.9°C and 1.4°C in 2090–2100, respectively. Global mean surface air temperatures are reduced by only 0.2°C in 2090–2100 in both scenarios when AOAM is implemented. Accordingly there is little potential for this method as a global CE measure, consistent with the previous results by *Cvijanovic et al*. [2015]. Therefore in the following, we focus on the Arctic defined as the region north of 70°N and all numbers given are averages over this region if not mentioned otherwise. The implementation of AOAM will be analyzed with respect to its potential to reduce Arctic warming and its impact on potential tipping elements discussed by *Lenton et al*. [2008] relative to the reference state in 2005–2015.

3.1. Arctic Radiation Balance and Temperature Changes

The albedo increase associated with the AOAM reduces the amount of shortwave radiation absorbed by the Arctic Ocean areas in summer. In the RCP8.5 (RCP4.5) AOAM simulations surface net downward shortwave radiation is reduced by maximum values of 82 (65) W m^{-2} in boreal summer by the end of the century relative to the default simulations without AOAM. This causes a cooling of the surface and consequently a decrease in the surface outgoing longwave radiation in the subsequent autumn of up to 16 (15) W m^{-2} compared to the default simulations. These changes in surface radiation fluxes cause a strong increase in upward net radiation at the top of the atmosphere (TOA). The two default RCP simulations show a negative 21st century trend in the upward TOA net radiation in the Arctic (Table 1), which is reversed if AOAM is implemented. The strongest effect is found for RCP8.5 simulations with an increase of net upward radiation at TOA by 62 W m^{-2} in the summers 2090–2100 upon the simulated deployment of AOAM. In the noEmit simulation no significant trend in TOA net radiation is evident. If AOAM is implemented in noEmit, radiative losses to space increase and temperatures decline.

Table 1. Arctic Climate System Changes for the Different Forcing Scenarios and Experiments[a]

Property	Total Value in 2005	RCP8.5	RCP8.5 AOAM	RCP4.5	RCP4.5 AOAM	noEmit	noEmit AOAM
TOA net upward radiation (W m^{-2})	121	−3.3	4.5	−1.2	3.9	0.4	3.8
Surface temperature (°C)	−13.3	4.4	3.2	2.2	1.2	−0.0	−0.6
Ocean ice volume (10^3km^3)	14.2	−7.7	−5.2	−4.2	−1.2	−0.5	1.6
Permafrost area (10^6km^2)	17.3	−8.1	−6.6	−4.0	−2.8	−0.1	0.7
Ocean albedo (1)	0.548	−0.104	0.065	−0.054	0.063	−0.005	0.070
Land albedo (1)	0.46	−0.048	−0.043	−0.029	−0.024	−0.004	−0.001

[a]The given differences are calculated from annual mean values between 2090–2100 and 2005–2015. The considered area is 70–90°N for all properties but for permafrost area and land albedo, where we consider the area of 50–90°N.

In 2005–2015 the simulated annual mean Arctic surface air temperature is −13.3°C (Table 1), followed by a positive annual mean temperature change until 2090–2100, which ranges between 4.4°C in the RCP8.5 simulation and 0.0°C in the noEmit simulation. With the exception of the noEmit simulations, for which the Arctic surface air temperature is reduced by 0.6°C in 2090–2100 relative to 2005–2015 under the deployment of AOAM, the warming trend in the Arctic can only partly be offset by AOAM. Within the first 5 years of AOAM deployment there is an initial decrease of Arctic surface air temperatures of 0.5°C, but thereafter Arctic temperatures start to increase again and follow the same trends as in the corresponding default simulations. The difference between the RCP8.5 and the RCP8.5 AOAM simulation at the end of the century is largest in autumn with lower temperatures of up to 4°C (and 3°C for RCP4.5) in the AOAM simulation.

Higher surface air temperatures cause an earlier spring melt of snow on land and a prolonged summer season, with a consequently higher rate of exposure to dark snow-free areas in summer [*Serreze and Barry*, 2011]. The annual mean land surface albedo in the 2005–2015 reference state north of 50°N is 0.46 (Table 1). In all six experiments this value decreases, meaning that more of the incoming shortwave radiation is absorbed. Hence the soils warm and emit more longwave radiation, further warming the atmosphere above. The AOAM simulations show lower land albedo decreases relative to their respective default simulations without AOAM (Table 1), because the lower temperatures in the AOAM simulations partly prevent the reduction of snow cover and changes in vegetation cover. Over the ocean, albedo changes are strongly related to sea ice. In the AOAM simulations, the annual mean albedo over the Arctic Ocean is forced to increase with respect to year 2005, in contrast to an oceanic albedo reduction in the default simulations (Table 1).

3.2. Arctic Sea Ice

The reduction of the Arctic surface temperatures achieved by AOAM is evaluated for its potential to reduce Arctic summer sea ice loss and to allow for the formation of thicker and therefore more robust winter sea ice. The simulated Northern Hemisphere annual minimum sea ice extent in the UVic ESCM amounts to 4.3 million km^2 in the summers of 2005–2015 (Figure 2a). This value is within the range of the summer sea ice extent simulated in the same time period by the CMIP5 models' of about 3 to 10 million km^2 [*Stroeve et al*., 2012], but lower than the observed minimum sea ice extent of about 5.5 million km^2 in 2005–2012 [*Stocker et al*., 2013]. The modeled mean September sea ice extent averaged over 2005–2014 is close to the observed sea ice extent in the same period (Figure 1, contour lines), although the simulated ice edge position differs slightly. In all three simulations without AOAM, the warming causes a decrease in the minimum sea ice extent until 2100. In the high emission RCP8.5 simulation only 1 million km^2 of the Arctic Ocean are still ice covered in summer, which is comparable to the CMIP5 mean of 0.5 million km^2 [*Stocker et al*., 2013]. The AOAM deployment causes a sea ice extent increase by about 0.75 million km^2 within the first 5 years after implementation, regardless of the emission scenario (Figure 2a). Thereafter the development of the minimum sea ice extent in the AOAM simulations follows very similar negative trends as the respective simulation without AOAM, i.e., a negative trend of 0.40 (0.12) million km^2 per decade for the RCP8.5 (RCP4.5) scenario and almost no trend in the noEmit simulations. This indicates that, after some positive effects in the first few years of implementation, AOAM is not able to prevent sea ice from decreasing in the longer term, as long as CO_2 continues to accumulate in the atmosphere. Nevertheless, the decline in Arctic sea ice cover is delayed in the simulations with AOAM: In the RCP8.5 (RCP4.5) case the implementation of AOAM causes the sea ice extent of 2100 to resemble the state of the default simulation of 2075 (2040). That is, AOAM may help to delay the effects of global warming by 25 (60) years with respect to Arctic sea ice decline under the RCP8.5 (RCP4.5) scenario.

In addition to sea ice extent, which is important for the radiation budget, sea ice thickness provides information about the robustness of the ice cover concerning short term temperature changes or weather fluctuations. The simulated annual modal ice thickness in the reference state of 2005 is 1.7 m, which agrees well with observed basin mean ice thicknesses of about 1.1 to 1.8 m for the same decade [*Lindsay and Schweiger*, 2015]. To get a better understanding of the development of the sea ice thickness distribution, we regard the initial sea ice thickness distribution of the Arctic Ocean in 2005 and its mean distribution for 2090–2100 for the six different experiments (Figure 2b). In 2005 the modal ice thickness is 1.7 m, with local maximum ice thicknesses reaching 5.1 m. As expected there is a shift toward thinner ice in the RCP8.5 simulation without AOAM, strongly reducing the amount of ice thicknesses larger than 1.5 m. The thickest ice toward the end of the 21^{st} century is only 3 m thick. In the RCP4.5 simulation without AOAM, the shift in sea ice thickness toward lower

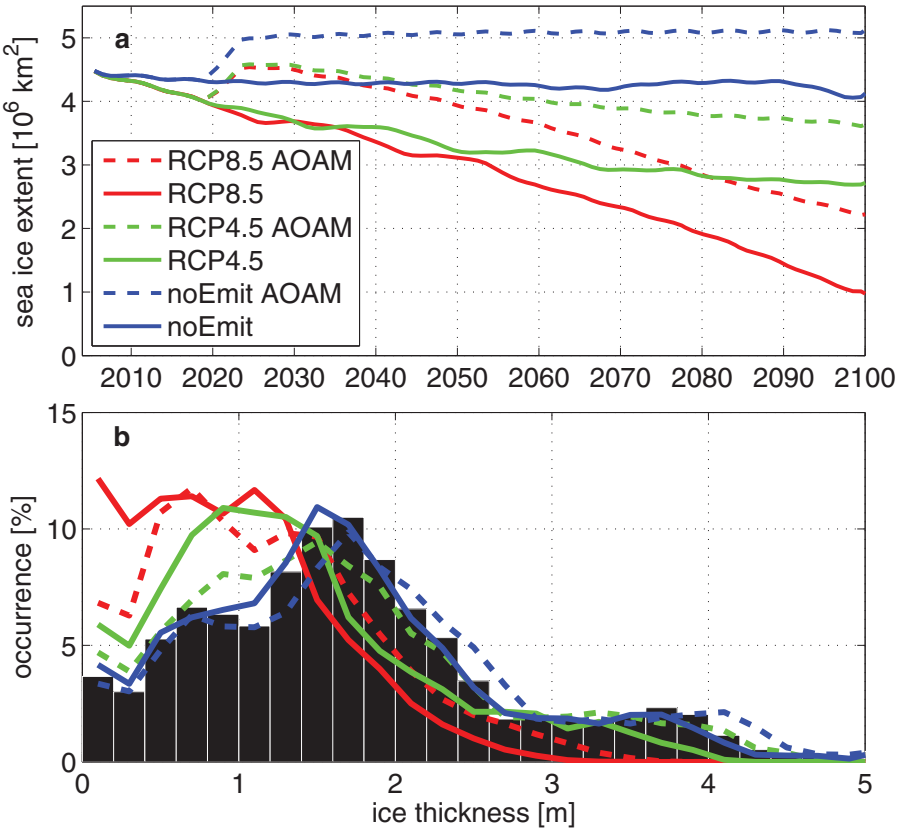

Figure 2. (a) Northern Hemisphere annual minimum sea ice extent for the different forcing scenarios, see legend, calculated as the yearly minimum of Arctic sea ice extent with a temporal resolution of 15 days; (b) Areal sea ice thickness distribution in the Arctic Ocean from 15 day mean value occurrences relative to total nonzero value occurrences in the year 2005 (black bars) and in the years 2090–2100 for the different forcing scenarios, color coding is the same as for Figure 2a.

values is also evident. The area with sea ice thicker than 1.7 m is strongly reduced and the maximum thickness is 3.9 m. Sea ice in the noEmit simulation without AOAM follows the distribution of the reference state in 2005 very closely.

AOAM causes the distribution to shift toward higher values. There is a more frequent occurrence of sea ice thicknesses larger than 1.5 m in the RCP8.5 AOAM simulation. For the RCP4.5 AOAM simulation the sea ice thickness distribution is very close to the 2005 distribution. An implementation of AOAM in the noEmit case accordingly causes the sea ice thickness distribution to shift to slightly higher values compared to the reference state.

In addition, in the high emission simulations without AOAM, the total Northern Hemisphere ice volume is strongly reduced by the end of the century. In the RCP8.5 (RCP4.5) simulation over 54 (30) % of the ice volume is lost (Table 1). This negative trend is only weakened and not reversed by the implementation of AOAM despite its positive effect on the ice thickness distribution. If we compare the ice volume in 2090–2100 to the reference state in 2005–2015, we see a larger decrease in the RCP8.5 AOAM simulation of 37%, compared to the default RCP4.5 simulation.

3.3. Meridional Overturning Circulation and Ocean Bottom Temperatures

The effects of AOAM on the radiation budget and sea ice coverage are generally consistent with findings of earlier studies [*Cvijanovic et al.*, 2015]. In the following, we thus focus on remote consequences of AOAM for the three-dimensional ocean circulation, water masses and heat transport. Generally, the Earth System regulates the meridional imbalance of the net radiation via meridional heat transports in the atmosphere and ocean. Climate model experiments suggest a weakening of the Atlantic Meridional Overturning Circulation

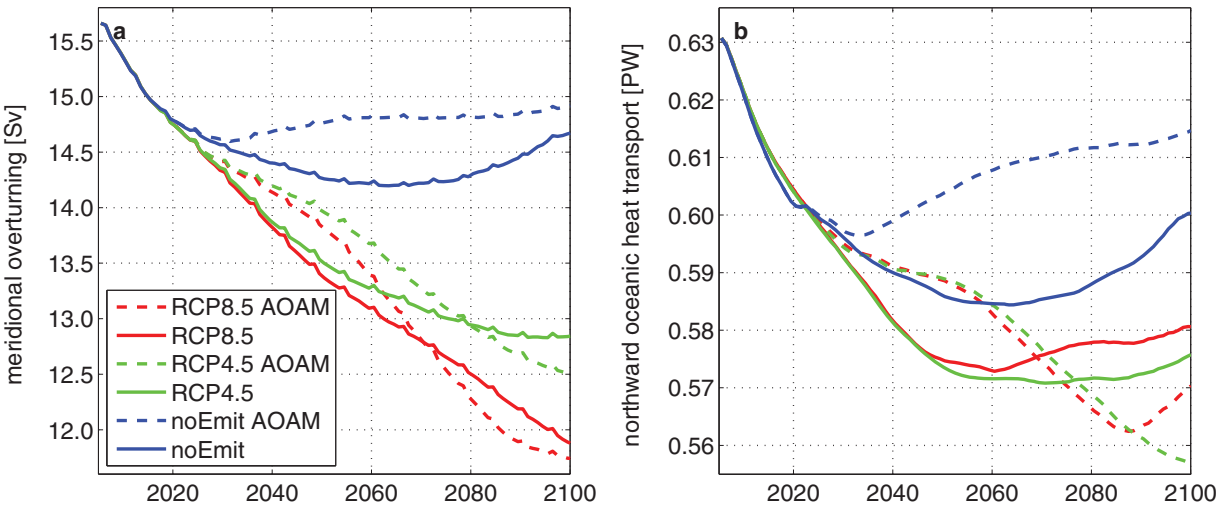

Figure 3. (a) Annual mean maximum North Atlantic meridional overturning and (b) annual mean northward oceanic heat transport in the Atlantic at 26°N for the different forcing scenarios and experiments, see legend.

(AMOC) under global warming conditions in response to a reduction in meridional temperature gradients resulting from Arctic amplification of global warming [*Stocker et al.*, 2013].

This negative trend is evident in the evolution of the AMOC in all three simulations without AOAM until 2050 (Figure 3a). A recovery of the AMOC is seen for the noEmit default simulation after 2070 and the decline has stopped in the RCP4.5 default simulation by 2100. In contrast, the AMOC strength keeps declining in the RCP8.5 simulation until 2100 because in this scenario atmospheric CO_2 concentrations still increase at the end of the century.

The reduction in high-latitude surface temperatures in the AOAM simulations causes the sea ice extent in the high northern latitudes to increase during the first 5 years of AOAM implementation (Figure 2a). The associated sea ice formation results in a salt flux into the ocean increasing the density of water exported from the Arctic ocean. This causes more intense deep convection in the subpolar North Atlantic between 50°N and 70°N, which is not temperature but salinity driven (supporting information Figure S2). As a consequence, a slower reduction of the AMOC is found in the experiments with AOAM between 2020 and about 2060 (Figure 3a). In the RCP8.5 and RCP4.5 AOAM simulations, the AMOC shows a stronger decrease after 2050, even stronger than in the default simulations without AOAM, which can again be attributed to changes in the freshwater budget in the North Atlantic deep convection areas. There is continued sea ice melt while regional precipitation does not change during this time period (supporting information Figure S2d). As a result, sea surface salinity in the North Atlantic area between 50 and 70°N is reduced between 2040 and 2080 (supporting information Figure S2c). As a result, the AMOC in the AOAM emission simulations show weaker overturning strengths compared to the respective default simulations in year 2100.

The initial delay in the AMOC reduction in the AOAM simulations causes a higher rate of northward heat transport from 2020 until 2060 compared to the default simulations (Figure 3b). For the period from 2005 to 2100 the accumulated northward heat transport in the AOAM simulation is higher by 0.021 PW for the RCP8.5 scenarios, whereas the increase is 0.228 PW for RCP4.5 and as high as 1.265 PW in the noEmit simulations.

The increased oceanic northward heat transport causes an unexpected subsurface warming in the AOAM simulations (Figure 4). In both RCP default simulations a surface warming, due to local heat exchange with the warming atmosphere in summer, and subsurface cooling are evident. The latter is associated with oceanic heat loss to the atmosphere during deep convection events in the Nordic Seas in winter and spring (Figure 5a). Note, in our model these convection sites extend to north of 70°N (supporting information Figure S3), and occur in addition to the main North Atlantic deep convection south of Iceland. Retreat of the winter sea ice edge due to progressing warming in the default emission scenarios enables open ocean

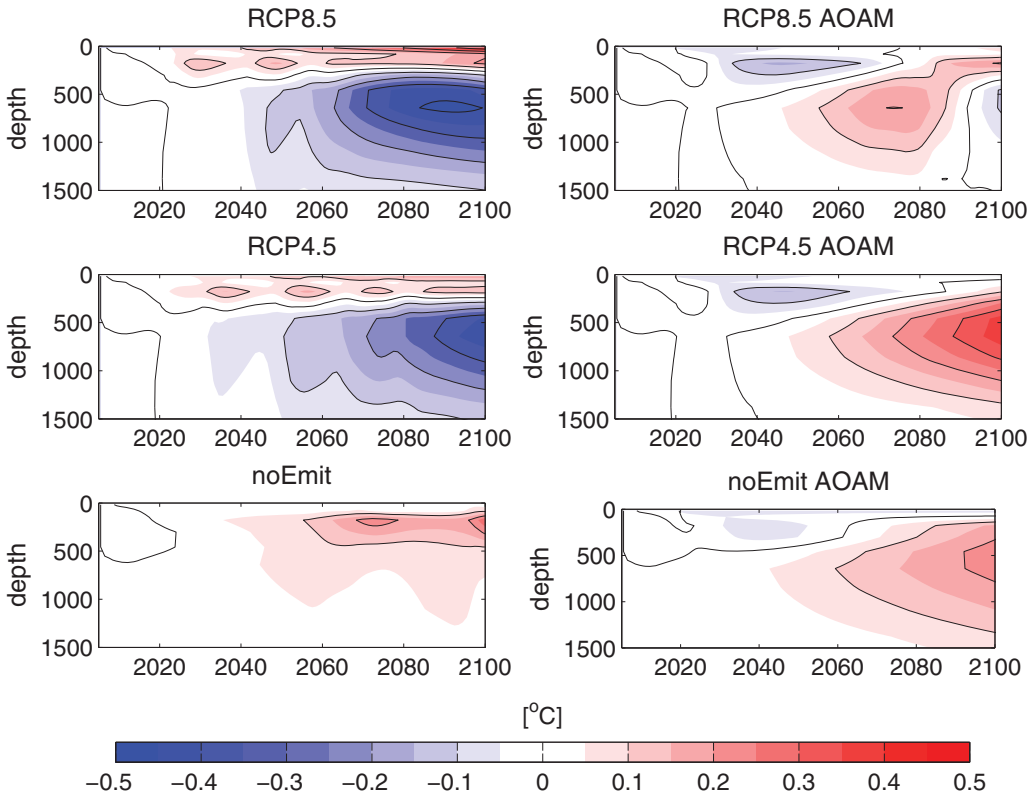

Figure 4. Hovmöller diagrams of mean Arctic vertical temperature profile changes relative to 2005 between 70 and 90°N for the six different forcing scenarios (left) and AOAM experiments (right). Black contours mark 0.1°C temperature intervals.

deep convection in this buoyantly unstable ocean area, which otherwise is prevented by a solid sea ice cover inhibiting direct exchange with the atmosphere. These events are much more unlikely to occur in the noEmit simulation, in which the ice cover does not retreat but nonetheless experiences natural variability.

In contrast, a subsurface warming signal is emerging at depths of 400–1200 m in the AOAM simulations, which is caused by two accompanying features. First, the lack of deep convection events in the AOAM simulations (Figure 5a), due to a winter sea ice cover which is forced to extent to 70°N, i.e., the location of the newly formed convection sites, prevents the deeper ocean from cooling. The RCP8.5 AOAM simulation is an exception, where deep convection occurs from 2080 onward, resulting in a cooling signal at the end of the century similar to the default runs. And second, water mass transport into the Arctic increases, which is evident from enhanced dilution of the implemented Arctic dye tracer (supporting information Figures S4 and S7). The dilution coincides with an increase in water temperatures, most notably at depths of 400–1200 m (Figure 5b and supporting information Figure S5). Note, that the entering water masses are again influenced by the heat exchange with the atmosphere (supporting information Figure S3), which explains the deep reaching negative temperature changes in the RCP8.5, RCP4.5 and NoEmit simulations. However, in the RCP8.5 AOAM and the RCP4.5 AOAM simulations, a warming signal in the entering water masses is evident, indicating a warming from entering water masses, uninfluenced by the deep convection. Increasing inflow to the Arctic always means warming as the entering water mass is always warmer, especially when there is no deep convection in the Nordic Seas. In addition the inflow water warms in the emission scenarios due to global warming.

Both the prevented deep convection and the increasing inflow lead to the subsurface warming signal located along the continental slope in the Arctic Ocean (Figure 6), where the effect of both features can be regarded separately. In the two RCP8.5 runs with and without AOAM, deep convection occurs continuously after 2080. Therefore, the warming signal along the continental shelf slope (Figure 6b) can be related to the temperature increase of the inflow from global warming. In contrast, the two RCP4.5 runs have opposing

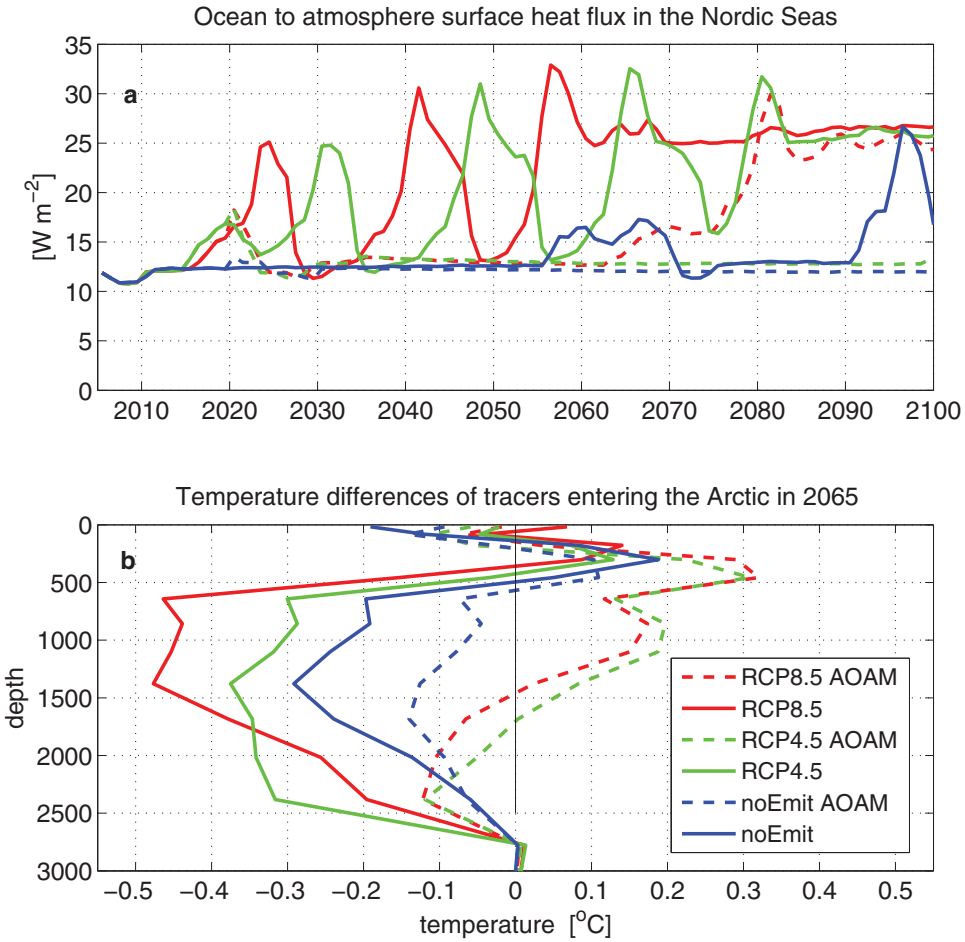

Figure 5. (a) Mean ocean to atmosphere surface heat flux in the Nordic Seas (defined as the area 65–80°N and 30°W to 30°E); (b) Temperature differences in traced water masses entering the Arctic for the different forcing scenarios and experiments, exemplarily for the period 2060–2070 relative to 2020–2025, i.e., the beginning of the tracer experiment.

deep convection states and we see en enhanced warming signal from accumulated heat due to the lack of deep convection in RCP4.5 with AOAM (Figure 6c). It is noteworthy that most of the Arctic marine methane hydrates are located along the slope of the continental margin [*Kvenvolden et al*., 1993; *Biastoch et al*., 2011]. A cooling trend as found in the default simulations would act to stabilize the hydrates. Our simulations indicate that introducing AOAM yields warming instead. We thus conclude that AOAM could increase the risk of melting methane hydrates, which could lead to a further increase in atmospheric greenhouse gas concentrations.

3.4. Permafrost Thawing

Increasing terrestrial temperatures in the Arctic can impact permafrost. The active layer in the upper meters of the soil is controlled by the annual mean air temperature and the amplitude of the seasonal cycle, while the actual temperature of the permafrost layer below is very close to the annual mean temperature [*Koven et al*., 2013]. In an attempt to assess the future development of permafrost, we take annual mean soil temperatures at 1 m depth below zero degrees Celsius as a simple indicator for the presence of permafrost. This estimate yields a simulated permafrost area of 17.6 million km^2 in 2005–2015 (Table 1 and Figure 7a). This is similar, though slightly lower, than the observational estimate by *Tarnocai et al*. [2009] with a permafrost area of 18.8 million km^2. In the UVic ESCM, the simulated soil temperature in the permafrost area of 2005–2015 increases by 1.2°C in the period from 1985 to 2015, which is in line with the observed trends of *Romanovsky et al*. [2013], who report that the permafrost temperature in Northern Russia has increased by 1–2°C over the last 30–35 years.

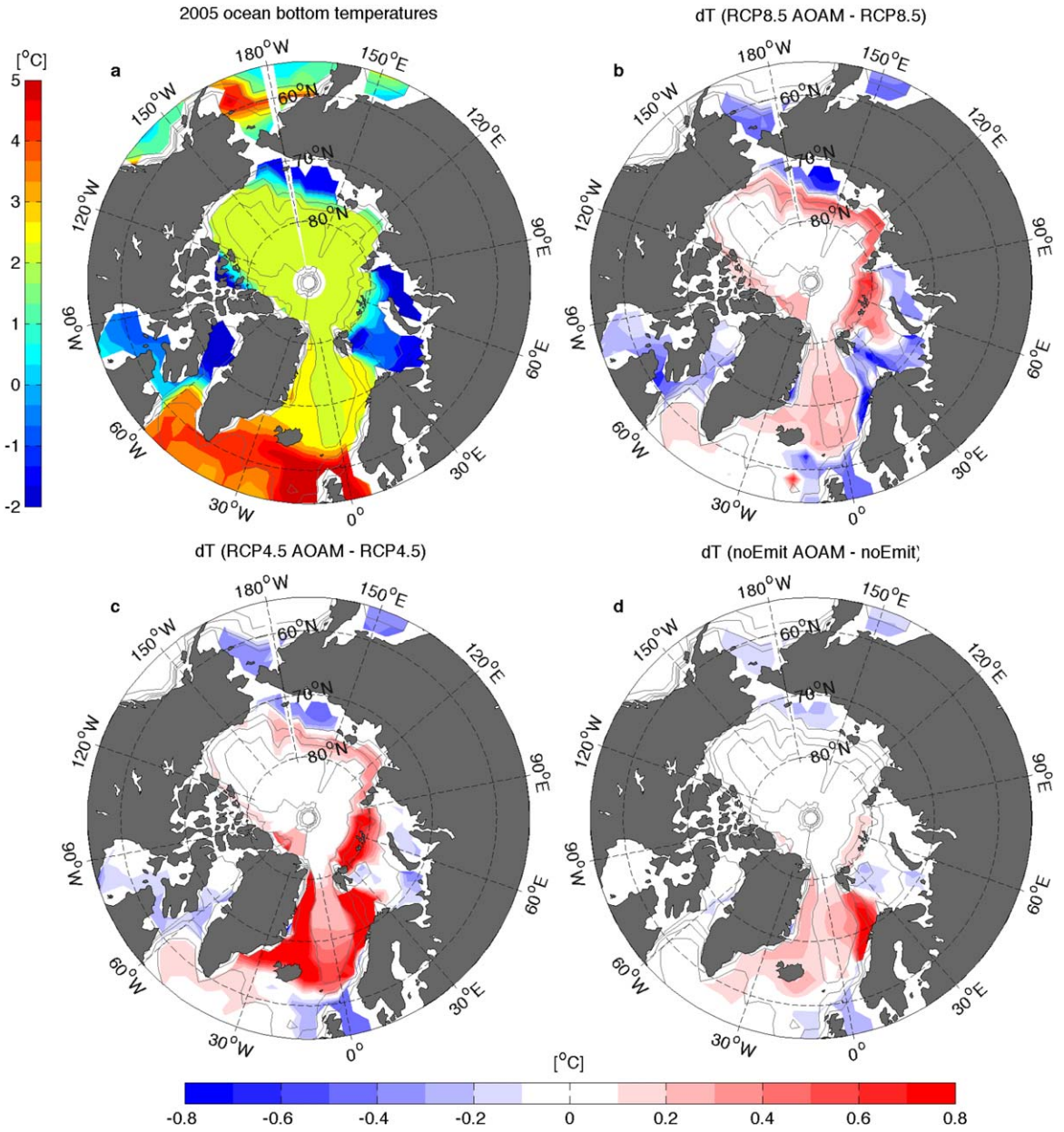

Figure 6. (a) Annual mean Arctic Ocean bottom temperatures simulated for 2005–2010; Annual mean changes in Arctic Ocean bottom temperatures in 2090–2100 due to the implementation of the AOAM in the (b) RCP8.5 simulation, (c) RCP4.5 simulation, and (d) noEmit simulation. Contour lines are model topography of 750 m, 1500 m and 2500 m depth.

Permafrost soil temperatures increase at 0.5 (0.2)°C per decade from 2020 to 2100 in the RCP8.5 (RCP4.5) scenario (Figure 7a). In the noEmit simulation temperatures in the permafrost soils start to stabilize at mean temperatures of about −5.6°C. As a consequence of increasing temperatures the permafrost area decreases in the two reference RCP simulations and the annual mean permafrost boundaries migrate northward (Figure 7b). In the default simulations under RCP8.5 (RCP4.5) the annual mean surface permafrost area is reduced by 8.9 (4.3) million km^2 by the end of the century. This is a reduction of 50.6 (24.4) % compared to the permafrost area in 2005–2015. For the noEmit simulation without AOAM the decrease by 2090–2100 is 1.1% of the 2005–2015 permafrost area.

AOAM delays the shrinking of the permafrost area. Since the positive temperature trends can not be reversed but only offset in the first few years of AOAM implementation, there is still an increasing soil temperature trend in the permafrost soils in the RCP8.5 (RCP4.5) AOAM simulations of 0.5 (0.1)°C per decade.

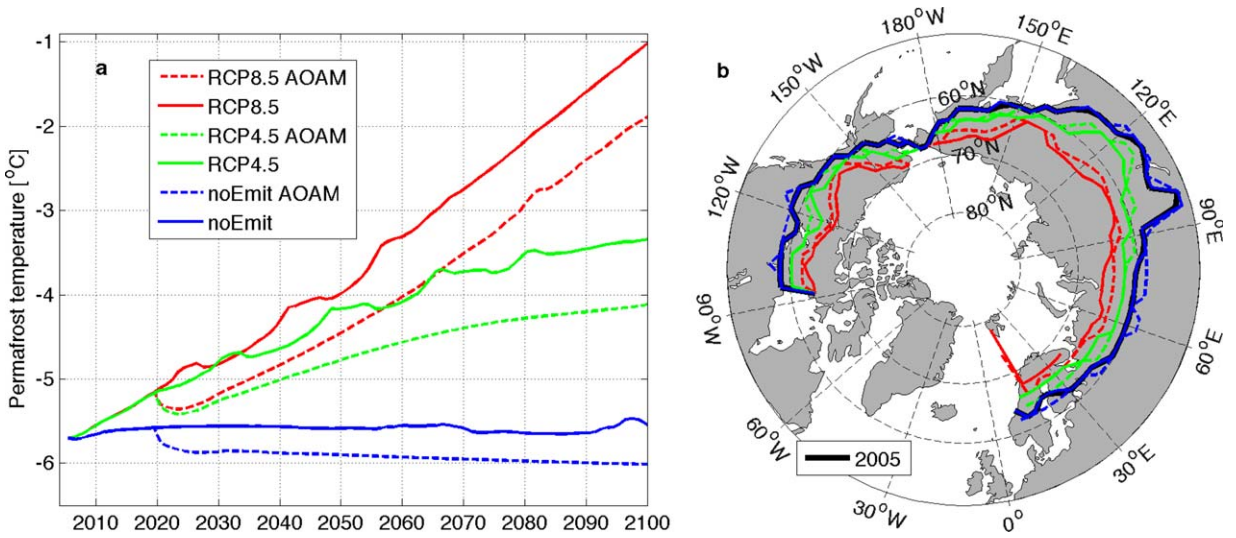

Figure 7. (a) Temporal development of the annual mean soil temperature in the uppermost meter in the area defined as permafrost in 2005–2015, see black border in Figure 7b for the different forcing scenarios; (b) map of annual mean permafrost boundaries in the years 2005–2015 (black) and in 2090–2100 for the different forcing scenarios and experiments, color coding is the same as for Figure 7a.

This initial offset in soil temperature trends relative to the default simulations, is reflected in larger surface area of annual mean permafrost in the AOAM simulations. For the noEmit AOAM simulation, the soil temperature trend is slightly negative, leading to a simulated expansion of permafrost area under AOAM.

Similar to surface air temperature and sea ice extent, soil temperatures highlight that AOAM only yields an initial onetime offset. Would this delay in surface warming still make a difference in terms of carbon release to the atmosphere? *Tarnocai et al*. [2009] provide estimates of soil carbon pools in the circumpolar permafrost area. Using their estimate of carbon content in the first meter of the soil of 26.4 kg m^{-2}, a prevented permafrost soil loss of about 1.7 (1.2) million km^2 until 2100 would amount to a prevented carbon release of 44.9 (31.7) Pg of carbon by 2100. These amounts correspond to about 3–4 years of today's annual carbon emissions and are small compared to the amount that would be released due to the permafrost area reduction in the reference RCP8.5 (RCP4.5) simulation of 235 (114) Pg C by 2100. Note, that these estimates are very simplistic and do not include feedbacks from the released carbon of the permafrost soils.

4. Discussion

4.1. Limitations of This Study

Some climatically important limitations of this study arise from the chosen model set up. With respect to the tipping elements of *Lenton et al*. [2008] and the Arctic radiation budget the most important ones are the treatment of the Greenland ice sheet, atmospheric chemistry and cloud processes. For the simulations in this study continental ice sheets were held constant to facilitate the interpretation of the results. While variations in ice sheet dynamics only play a marginal role during the 100 year period studied, the lack of simulated melting from the Greenland ice sheet will cause a bias in the simulated freshwater input to the North Atlantic Ocean. The melt water would likely cause a reduction in deep water formation due to increased vertical stratification and thus could potentially interfere with a recovery of the AMOC as initially seen upon implementation of AOAM in the model. On the other hand, AOAM causes a reduction in surface air temperatures as well as ocean surface temperatures around Greenland, and could therefore possibly reduce Greenland ice melt. It is beyond the scope of this study to investigate, which of these processes is dominant on different time scales.

The UVic ESCM does not include atmospheric chemistry. Thus we cannot investigate whether or not a cooling of the ocean surface would favor, for example, ozone depletion in the stratosphere and potentially impact the Arctic ozone hole. We can only speculate, that the changes in meridional temperature gradients due to the implementation of AOAM might influence atmospheric circulation patterns and thereby might

affect ozone depletion. However, AOAM is implemented mostly during summer, and chemical ozone depletion takes place in winter/spring. We therefore expect no strong interference between these two processes.

Further limitations of our study include the coarse resolution of our model, the simplistic representation of the atmosphere and the lack of a more sophisticated permafrost model. Due to the coarse resolution grid, our model simulates North Atlantic deep convection not at the observed location in the Labrador Sea, but further east, south of Iceland. This bias does not have a strong impact on the results of this study concerning the changes in the deep convection, since these are forced by changes in sea surface salinity, which occur everywhere in the Atlantic between 50 and 70°N. However, it is noteworthy that salinity in the western part of the North Atlantic in our model are in general lower, and might therefore be more sensitive to changes in sea surface salinity. The UVic ESCM lacks a vertical representation of atmospheric dynamics and does not simulate a dynamic cloud response. Therefore, the model misses part of the changes in meridional heat and moisture transports [*Graversen et al*., 2008] and lacks the cloud-albedo feedback as described by *Serreze and Barry* [2011]. Other atmospheric feedbacks such as the response of sensible and latent heat fluxes as well as the longwave radiation response are however implemented. Furthermore, our estimate of soil permafrost is a simple calculation lacking the dynamical representation of vertical soil temperature profiles as used by, e.g., *Avis et al*. [2011] and *MacDougall et al*. [2012].

4.2. Assessment of AOAM

We assess the potential of AOAM in light of the Arctic tipping elements described by *Lenton et al*. [2008] under varying CO_2 emission scenarios: In line with *Cvijanovic et al*. [2015] we find a limited potential in global temperature reduction. However, Arctic surface air temperatures in 2090–2100 can be reduced by 1.2°C in the RCP8.5 AOAM simulation relative to the default emission simulation, which is comparable to the regional 1.6°C temperature reduction found by *Cvijanovic et al*. [2015] in an experiment with an albedo modification of 0.8 over the area north of 70°N, i.e., the same AOAM implementation, but with different CO_2 forcing.

In all AOAM simulations, Arctic summer sea ice area can initially be increased by 0.75 million km^2, but then continues to follow the negative trend of the respective default simulation. In 2090–2100, 53% of the 2005–2015 summer sea ice area remains in the RCP8.5 AOAM simulation, compared to 27% of the ice area remaining in the RCP8.5 simulation. Our values are higher compared to the 29% remaining summer sea ice cover from the study of *Cvijanovic et al*. [2015, their experiment: albedo of 0.8 north of 70°N], since we use different reference states, namely 2005–2015 in our study, compared to a preindustrial 1xCO_2 atmosphere reference in the study by *Cvijanovic et al*. [2015], as well as different averaging areas.

In contrast to the study by *Cvijanovic et al*. [2015] focusing on atmospheric variables, we here focus on oceanic and terrestrial processes. All AOAM simulations reveal a potential to initially increase the strength of the AMOC relative to the default simulations. A side effect of the associated initial higher northward oceanic heat transport in the AOAM simulations compared to the default simulations is a subsurface warming located along the continental slope. This is the region where most of the Arctic marine methane hydrates are located [*Kvenvolden et al*., 1993; *Biastoch et al*., 2011]. Our results indicate that the partial recovery of the AMOC, which is one of the potential tipping elements from *Lenton et al*. [2008], as well as the inhibited deep convection is favoring a destabilization of the marine methane hydrates in the Arctic, another listed potential tipping element discussed by *Lenton et al*. [2008]. This trade off illustrates that it might not be possible to simultaneously address all Arctic tipping elements with such a local CE measure.

Nevertheless, an initial offset of the positive temperature trends yields some potential in reducing the risk of releasing additional greenhouse gases to the atmosphere. Until 2100 this offset leads to a prevented carbon release from melting permafrost soils of 19 (28) % in the RCP8.5 (RCP4.5) AOAM simulation relative to the default simulations without AOAM. *Cvijanovic et al*. [2015] show that about 40% of the preindustrial permafrost area remains in their model simulations. In our RCP8.5 AOAM simulation 59% of the 2005–2015 permafrost area remains frozen.

Furthermore we find that with progressing climate change, deep convection events start to occur in the Nordic Seas in the default emission simulations, and act to cool the deep ocean. These convection events are initially prohibited by the implementation of AOAM. Since the newly formed deep convection areas are located right at the edge of the 70°N border, i.e., the AOAM implementation border in the Nordic seas,

where with progressing climate change the sea ice starts to retreat if AOAM is not implemented. This hints to the fact that the Arctic climate system reacts sensitive to the location of the AOAM implementation.

In contrast to the study by *Cvijanovic et al*. [2015], our transient climate change setting enables us to look at changes in simulated trends of the various metrics. It is found that, AOAM has no potential to reverse trends in Arctic surface air temperature, sea ice and soil temperatures, but rather holds some potential to temporarily offset these trends. This holds true for all simulations, including a high emission scenario as well as a very idealized maximum mitigation scenario (excluding negative emissions). In line with the fact that a local cooling at high northern latitudes causes compensatory heat fluxes in the atmosphere and the ocean [*Tilmes et al*., 2013], the regulation of internal heat budgets in the climate system limits the potential of AOAM to counteract Arctic amplification of global warming. Moreover, we find that no matter when the deployment of AOAM is terminated even under the intermediate emission scenario RCP4.5, the sea ice extent quickly reverses to match the sea ice extent of the default simulation (supporting information Figure S6). This demonstrates how AOAM must be maintained over decades to keep up its initial effect of delaying global warming consequences in the Arctic.

5. Conclusion

The self-regulating nature of the climate system prevents regional, high latitude CE methods from having global and sustainable effects. In line with *Tilmes et al*. [2013] we find that the Arctic cooling introduced by AOAM causes compensatory meridional heat transports, limiting the effect of AOAM to a single, nonrepeatable delay of the warming, sea ice loss and permafrost retreat if greenhouse gas emissions continue to rise. Moreover, undesirable side effects arise from the potential of enhanced warm water inflow into the Arctic Ocean to destabilize methane hydrates. In this respect AOAM could even increase the risk of releasing additional, natural greenhouse gases to the atmosphere.

At the end of the 21st century the state of the intermediate emission simulation (RCP4.5) without AOAM is closer to the 2005–2015 reference state than the state of the high emission scenario (RCP8.5) with AOAM applied, for all metrics considered. This demonstrates that AOAM only delays impacts of ongoing CO_2 emissions. Thus on longer time scales a reduction in emissions still appears to be the safest way to prevent severe climate change in the Arctic.

Acknowledgments
The model data used to generate the table and the figures will be made available at http://thredds.geomar.de. We thank Christina Roth, Julia Getzlaff and Heiner Dietze for helpful discussions. This work was funded by the German DFG in the context of the Priority Program Climate Engineering: Risks, Challenges, Opportunities? (SPP 1689). The authors declare that they have no competing financial interests. N.M., A.O. and D.P.K. conceived and designed the experiments. N.M. implemented and performed the experiments and analyzed the data. N.M. wrote the manuscript with contributions from D.P.K., T.M. and A.O. The authors would like to thank Ivana Cvijanovic, an anonymous reviewer, and the associate editor for their helpful and constructive comments, and the editorial staff for their efforts.

References

Avis, C. A., A. J. Weaver, and K. J. Meissner (2011), Reduction in areal extent of high-latitude wetlands in response to permafrost thaw, *Nat. Geosci.*, *4*(7), 444–448, doi:10.1038/ngeo1160.

Biastoch, A., et al. (2011), Rising Arctic Ocean temperatures cause gas hydrate destabilization and ocean acidification, *Geophys. Res. Lett.*, *38*, L08602, doi:10.1029/2011GL047222.

Bitz, C. M., M. M. Holland, A. J. Weaver, and M. Eby (2001), Simulating the ice-thickness distribution in a coupled climate model, *J. Geophys. Res.*, *106*, 2441–2463.

Blackstock, J. J., D. S. Battisti, K. Caldeira, D. M. Eardley, J. I. Katz, D. W. Keith, A. A. N. Patrinos, D. P. Schrag, R. H. Socolow and S. E. Koonin (2009), Climate engineering responses to climate emergencies. [Available at http://arxiv.org/pdf/0907.5140.]

Caldeira, K., and L. Wood (2008), Global and Arctic climate engineering: Numerical model studies, *Philos. Trans. R. Soc. A*, *366*, 4039–4056, doi:10.1098/rsta.2008.0132.

Crook, J. A., L. S. Jackson, and P. M. Forster (2016), Can increasing albedo of existing ship wakes reduce climate change?, *J. Geophys. Res. Atmos.*, *121*, 1549–1558, doi:10.1002/2015JD024201.

Crutzen, P. (2006), Albedo enhancement by stratospheric sulfur injections: A contribution to resolve a policy dilemma?, *Clim. Change*, *77*, 211–219, doi:10.1007/s10584-006-9101-y.

Cvijanovic, I., K. Caldeira and D. G. MacMartin (2015), Impacts of ocean albedo alteration on Arctic sea ice restoration and Northern Hemisphere climate, *Environ. Res. Lett.*, *10*, 1–8, doi:10.1088/1748-9326/10/4/044020.

Eby, M. et al. (2013), Historical and idealized climate model experiments: An intercomparison of Earth system models of intermediate complexity, *Clim. Past*, *9*, 1111–1140, doi:10.5194/cp-9-1111-2013.

Evans J. R. G., E. P. J. Stride, M. J. Ediringhe, D. J. Andrews, and R. R. Simons (2010), Can oceanic foams limit global warming?, *Clim. Res.*, *42*, 155–160, doi:10.3354/cr00885.

Fanning, A. F., and A. J. Weaver (1996), An atmospheric energy-moisture balance model: Climatology, interpentadal climate change, and coupling to an ocean general circulation model, *J. Geophys. Res.*, *101*, 15,111–15,128, doi:10.1029/96JD01017.

Feichter, J., and T. Leisner (2009), Climate engineering: A critical review of approaches to modify the global energy balance, *Eur. Phys. J. Spec. Top.*, *176*, 8192, doi:10.1140/epjst/e2009-01149-8.

Gordon, A., and N. Walter (2011), Controlling the Earths albedo using reflective hollow glass spheres, *Int. J. Global Environ. Issues*, *11*(2), 91–108.

Graversen, R. G., T. Mauritsen, M. Tjernstrom, E. Kallen, G. Svensson (2008), Vertical structure of recent Arctic warming, *Nature*, *451*, 53–56, doi:10.1038/nature06502.

Holland, M. M., and C. M. Bitz (2003), Polar amplification of climate change in coupled models, *Clim. Dyn.*, *21*, 221–232, doi:10.1007/s00382-003-0332-6.
Hulme, M. (2014), *Can Science Fix Climate Change? A case Against Climate Engineering*, Polity Press, Cambridge, U. K.
Hunke E. C., and J. K. Dukowicz (1997), An elastic-viscous-plastic model for sea ice dynamics, *J. Phys. Oceanogr.*, *27*, 1849–1867.
Jin, Z., T. P. Charlock, W. L. Smith Jr., and K. Rutledge (2004), A parameterization of ocean surfacealbedo, *Geophys. Res. Lett.*, *31*, L22301, doi:10.1029/2004GL021180.
Keith, D. W. (2013), *A Case for Climate Engineering*, MIT Press, Cambridge, Mass.
Keller, D. P., A. Oschlies, and M. Eby (2012), A new marine ecosystem model for the University of Victoria Earth system climate model, *Geosci. Model Dev. Discuss.*, *5*(2), 1135–1201.
Keller, D. P., E. Y. Feng, and A. Oschlies (2014), Potential climate engineering effectiveness and side effects during a high carbon dioxide-emission scenario, *Nat. Commun.*, *5*, 1–11, doi:10.1038/ncomms4304.
Koven, C. D., W. J. Riley and A. Stern (2013), Analysis of permafrost thermal dynamics and response to climate change in the CMIP5 Earth System Models, *J. Clim.*, *26*(6), 1877–1900.
Kvenvolden K. A., G. D. Ginsburg, and V. A. Soloviev (1993), Worldwide distribution of subaquatic gas hydrates, *Geo Mar. Lett.*, *13*, 32–40.
Lenton, T. M. (2012), Arctic climate tipping points, *Ambio*, *41*(1), 10–22, doi:10.1007/s13280-011-0221-x.
Lenton T. M., H. Held, E. Kriegler, J. W. Hall, W. Lucht, S. Rahmstorf and H. J. Schellnhuber (2008), Tipping elements in the Earth's climate system, *Proc. Natl. Acad. Sci. U. S. A.*, 1786–1793, doi:10.1073/pnas.0705414*105*.
Lindsay, R., and A. Schweiger (2015), Arctic sea ice thickness loss determined using subsurface, aircraft, and satellite observations, *Cryosphere*, *9*, 269–283, doi:10.5194/tc-9-269-2015.
MacCracken, M. C., H.-J. Shin, K. Caldeira and G. A. Ban-Weiss (2013), Climate response to imposed solar radiation reductions in high latitudes, *Earth Syst. Dyn.*, *4*, 301–315, doi:10.5194/esd-4-301-2013.
MacDougall, A. H., C. A. Avis and A. J. Weaver (2012), Significant contribution to climate warming from the permafrost carbon feedback, *Nat. Geosci.*, *5*, 719–721, doi:10.1038/NGEO1573.
Meier, W., F. Fetterer, M. Savoie, S. Mallory, R. Duerr, and J. Stroeve (2013), *NOAA/NSIDC Climate Data Record of Passive Microwave Sea Ice Concentration, Version 2*, Natl. Snow and Ice Data Cent., Boulder, Colo., doi:10.7265/N55M63M1.
Meinshausen, M., et al. (2011), The RCP greenhouse gas concentrations and their extensions from 1765 to 2300, *Clim. Change*, *109*(1-2), 213–241.
Meissner, K. J., A. J. Weaver, H. D. Matthews, and P. M. Cox (2003), The role of land surface dynamics in glacial inception: A study with the UVic Earth System Model, *Clim. Dyn.*, *21*(7-8), 515–537.
Pacanowski, R. C. (1995), MOM 2 documentation, users guide and reference manual, *Tech. Rep. 3*, GFDL Ocean Group, Geophys. Fluid Dyn. Lab., Princeton, N. J.
Perovich, D. K., T. C. Grenfell, B. Light, and P. V. Hobbs (2002), Seasonal evolution of the albedo of multiyear Arctic sea ice, *J.Geophys. Res.*, *107*(C10), 8044, doi:10.1029/2000JC000438.
Robock, A. (2008), 20 reasons why geoengineering may be a bad idea, *Bull. At. Sci.*, *64*(2), 14-18, 59, doi:10.2968/064002006.
Robock, A., L. Oman, and G. L. Stenchikov (2008), Regional climate responses to geoengineering with tropical and Arctic SO_2 injections, *J. Geophys. Res.*, *113*, D16101, doi:10.1029/2008JD010050.
Romanovsky, V. E., S. L. Smith, H. H. Christiansen, N. I. Shiklomanov, D. A. Streletskiy, D. S. Drozdov, N. G. Oberman, A. L. Kholodov, and S. S. Marchenko (2013), Permafrost [in Arctic Report Card 2013]. [Available at http://www.arctic.noaa.gov/report13/ArcticReportCard_full_report.pdf.]
Screen, J. A., and I. Simmonds (2010), The central role of diminishing sea ice in recent Arctic temperature amplification, *Nature*, *464*(7293), 1334–1337.
Seitz R. (2011), Bright water: Hydrofoils, water conservation and climate change, *Clim. Change*, *105*, 365–381, doi:10.1007/s10584-9965-8.
Serreze, M. C., and R. G. Barry (2011), Processes and impacts of Arctic amplification, *Global Planet. Change*, *77*, 85–96, doi:10.1016/j.gloplacha.2011.03.004.
Serreze, M. C., and J. A. Francis (2006), The Arctic amplification debate, *Clim. Change*, *76*, 241–264
Skvortsov A., M. Eby, and A. Weaver (2009), Snow cover validation and sensitivity to CO2 in the UVic ESCM, *Atmos. Ocean*, *47*(3), 224–237, doi:10.3137/AO929.2009.
Stocker, T. F., D. Qin, G.-K. Plattner, M. Tignor, S. K. Allen, J. Boschung, A. Nauels, Y. Xia, V. Bex and P. M. Midgley (Eds.) (2013), *IPCC, 2013: Climate Change 2013: The Physical Science Basis. Contribution of Working Group I to the Fifth Assessment Report of the Intergovernmental Panel on Climate Change*, 1535 pp., Cambridge Univ. Press, Cambridge, U. K.
Stroeve, J. C., V. Kattsov, A. Barrett, M. Serreze, T. Pavlova, M. Holland, and W. N. Meier (2012), Trends in Arctic sea ice extent from CMIP5, CMIP3 and observations, *Geophys. Res. Lett.*, *39*, L16502, doi:10.1029/2012GL052676.
Tarnocai, C., G. Canadell, E. A. G. Schuur, P. Kuhry, G. Mazhitova, and S. Zimov (2009), Soil organic carbon pools in the northern circumpolar permafrost region, *Global Biogeochem. Cycles*, *23*, GB2023, doi:10.1029/2008GB003327.
Taylor K. E., R. J. Stouffer, and G. A. Meehl (2012), An overview of CMIP5 and the experimental design, *Bull. Am. Meteorol. Soc.*, *41*, 485–498, doi:10.1175/BAMS-D-11-00094.1.
Tietsche, S., D. Notz,J. H. Jungclaus, and J. Marotzke (2011), Recovery mechanisms of Arctic summer sea ice, *Geophys. Res. Lett.*, *38*, L02707, doi:10.1029/2010GL045698.
Tilmes, S., A. Jahn, J. E. Kay, M. Holland, and J. F. Lamarque (2013), Can regional climate engineering save the summer Arctic sea ice?, *Geophys. Res. Lett.*, *41*, 880–885, doi:10.1002/2013GL058731.
Wadhams, P. (2012), Arctic ice cover, ice thickness and tipping points, *Ambio*, *41*(1), 23–33, doi:10.1007/s13280-011-0222-9.
Weaver, A. J., et al. (2001), The UVic earth system climate model: Model description, climatology, and applications to past, present and future climates, *Atmos. Ocean*, *39*, 361–428, doi:10.1080/07055900.2001.9649686.